Postprint of: Kowalska E., Janczarek M., Rosa L., Juodkazis S., Ohtani B., Mono- and bi-metallic plasmonic photocatalysts for degradation of organic compounds under UV and visible light irradiation, Catalysis Today, Vol. 230 (2014), pp. 131-137, DOI: 10.1016/j.cattod.2013.11.021

Mono- and bi-metallic plasmonic photocatalysts for degradation of organic compounds under UV and visible light irradiation

E. Kowalska[a,*], M. Janczarek[a,b], L. Rosa[c], S. Juodkazis[c], B. Ohtani[a]

[a] Catalysis Research Center, Hokkaido University, N21, W10, 001-0021, Sapporo, Japan
[b] Department of Chemical Technology, Gdansk University of Technology, 80-233 Gdansk, Poland
[c] Swinburne University of Technology, PO Box 218, Hawthorn, 3122 Australia

* Corresponding author. Tel.: +81 117069130.
E-mail address: kowalska@cat.hokudai.ac.jp (E. Kowalska).

Abstract

Titania powders were surface modified with gold and/or silver nanoparticles (NPs) by photodeposition method. Gold modified titania exhibited much higher photocatalytic activity during methanol dehydrogenation under UV irradiation than titania modified with monometallic silver and bimetallic Au-Ag NPs. Bimetallic photocatalysts exhibited either enhanced or reduced visible light activity, depending on properties of noble metal NPs, sequence of their deposition on titania, and properties of host titania. Though numerical simulation (3D-FDTD) showed strong plasmonic field enhancement at the interface between titania and bimetallic core(Au)-shell(Ag) NP, it is thought that co-deposition caused an enhancement of charge carriers recombination (by electron sinking in nearby second metal) inhibiting photoactivity under visible light irradiation. The highest level of photoactivity showed large rutile NPs with successively deposited metals, mainly in the form of individual monometallic NPs, due to size/shape polydispersity of deposited NPs, and thus with ability of light absorption in a broad wavelength range.

Keywords

3D-FDTD simulations; bimetallic photocatalyst; gold and silver nanoparticles; plasmonic photocatalyst; titania; visible-induced photoactivity

1. Introduction

Sufficient energy, clean environment and safe drinking water belong to three of the top ten humanity's problems for the next 50 years [1]. Therefore, a lot of efforts have been made to develop new technologies for efficient and cheap energy production and water/wastewater treatment. Application of solar radiation, and thus solar induced photocatalysis may be one of the future technologies overcoming these problems. Titania (titanium(IV) oxide, TiO_2) has been one of the most investigated photocatalysts during the past forty years, due to its high photocatalytic activity, redox properties, thermal and chemical stability and non-toxicity [2-5].

The limitation in its application, resulting from low quantum yield (fast recombination of charge carriers: e^-/h^+) and necessity to use UV irradiation, may be overcome since modified titania often possesses higher activity and ability of working under visible-light irradiation [6, 7]. Large variety of organic and inorganic compounds have been examined as dopants or surface modifiers, among them noble metals, since they enhance the transfer of photogenerated electrons prolonging charge carriers lifetime [8-10]. Some of them, exhibiting plasmonic properties (localized surface plasmon resonance, LSPR), such as gold and silver, may also activate wide band gap semiconductors (TiO_2, CeO_2) towards visible-light [11, 12]. Recently we have shown that the activity of gold modified titania (Au@TiO_2) under visible-light irradiation depends on titania and gold properties, and photocatalysts with ability of light absorption in a wide wavelength range (broad LSPR peak) showed the highest level of activity as a result of utilization of large amount of incident photons [13, 14]. Nano-architecture arrangement (shape and size of noble metal) as well as selection of noble metal and titania form may allow preparing the photoactive catalysts under overall solar spectrum. Recently, improved photoactivity under visible light irradiation has been reported for modified titania with bimetallic silver and gold NPs prepared by microemulsion method [15].

It must be pointed that function of noble metal is different under UV and visible light irradiation. Under UV irradiation titania is activated and photo-generated electrons sink in NPs of noble metal, hindering the recombination of charge carriers (e^-/h^+), which results in activity increase [16, 17]. Under visible light irradiation titania cannot be activated (band-gap: 3-3.2 eV), and thus light must be absorbed by plasmonic NPs. Two possible mechanisms of titania activation by plasmonic NPs under visible light irradiation have been recently proposed, *i.e.* charge [11] and energy transfer [18]. In the present study we have examined bimetallic titania photocatalysts prepared by successive and simultaneous (co-) photodeposition and discussed the mechanism of organics decomposition under visible light irradiation.

2. Material and methods

2.1 Photocatalyst preparation

2.1.1 Monometallic photocatalyst

2 wt% of gold or silver, which corresponds to 0.81 and 1.48 mol% to titania, respectively, was photodeposited on the surface of four commercial photocatalysts composed of rutile (TIO-6 from Catalysis Society of Japan and Ald_R from Aldrich) and anatase (ST-41 and ST-01 from Ishihara) forms of titania (Au@TiO_2, Ag@TiO_2) by procedure briefly described below. Titania powder (572 mg) was suspended in 28.6 mL 50vol% aqueous methanol solution in a pyrex tube. Then 598 or 450 μL of $HAuCl_4 \cdot 4H_2O$ or $AgNO_3$ aqueous solution (0.097 or 0.23 M) was added to the tube for god or silver deposition, respectively. The tube was purged of air with argon for at least 15 min and then sealed with a rubber septum. The absence of oxygen in the tube was checked by injection of 0.2 mL gas sample into a gas chromatograph with thermal conductivity detector (GC-TCD, Shimadzu GC8A-IT). The suspension was photoirradiated with a 400-W high-pressure mercury lamp (Eiko-sha) under magnetic stirring (500 rpm). The temperature of the suspension during photoirradiation was maintained at 298 ± 5 K using a thermostatically controlled water bath. During the irradiation, the amount of generated hydrogen was measured every 15 min by injection of 0.2 mL gas sample into a gas chromatograph (the same as for O_2 checking). The thus-obtained photocatalyst was centrifuged, washed with methanol and at least three times with distilled water, dried overnight at 393 K, and ground in an agate mortar.

2.1.2 Bimetallic photocatalyst

2 wt% of gold and 2 wt% of silver was photodeposited on the surface of three commercial titania photocatalysts: rutile (TIO-6, Ald_R) and anatase (ST-41). Two kinds of deposition were applied: i) simultaneous deposition (co-deposition) of gold and silver (Au&Ag@TiO_2) and ii) successive deposition of one metal on the surface of formerly modified titania with another metal, *i.e.* Ag@(Au@TiO_2) – silver was deposited on gold modified titania (Au@TiO_2), and Au@(Ag@TiO_2) – gold was deposited on silver modified titania (Ag@TiO_2).

The photodeposition conditions were the same as in the case of monometallic photodeposition.

2.2 Photocatalyst characterization and photoactivity tests

The plasmonic titania powders were characterized by diffuse reflectance spectroscopy (DRS), scanning transmission electron microscopy (STEM, Hitachi, HD2000 ultrathin film evaluation system), X-ray powder diffraction (XRD) [14], and X-ray photoelectron spectroscopy (XPS, JEOL JPC-9010MC using Mg Kα X-ray).

The photocatalytic activity was examined during methanol dehydrogenation (50% MeOH, argon) under UV irradiation (Hg lamp) and 2-propanol oxidation (5 vol%) under visible light irradiation (Xe lamp, $\lambda > 450$ nm) using previously described irradiation set-ups [14].

2.3 Numerical simulation of LSPR

The influence of titania modification with a different noble metal was performed by numerical simulations using finite difference time domain method 3D-FDTD (Lumerical software). The plasmonic resonance was calculated for a spheroidal Au NP with 10 nm diameter and 30 nm height, touching the substrate (titania) and covered by a layer of silver, which itself ends flat on the substrate, for a thickness t of 2 and 5 nm around the gold NP.

3. Results and Discussion

3.1 Photocatalyst preparation

Plasmonic photocatalysts were prepared by photodeposition method in the presence of methanol as a sacrificial hole scavenger. The course of alcohol dehydrogenation, measured by hydrogen evolution, indicates complete metal deposition when continuous liberation of hydrogen at a constant rate is observed [19]. It must be pointed that the presence of noble metal NPs is necessary for hydrogen generation and no alcohol dehydrogenation has been observed on bare titania, proving that protons are reduced on the surface of co-catalyst, *i.e.* noble metal NPs [8, 9, 16, 20]. In the case of monometallic photocatalysts, the induction period precedes continuous hydrogen evolution, during which metal cations are reduced to metallic NPs. An example of metal deposition on bare or monometallic-modified rutile titania of small primary

particle size (PPS=15 nm, TiO_2=TIO-6, BET=100 m^2g^{-1} [21]) is shown in Figure 1, left. In the case of monometallic photocatalysts (Au@TiO_2, Ag@TiO_2; TiO_2=TIO-6), much shorter induction period for gold (4 min, dashed line) than for silver (30 min) indicates its higher photo-reduction ability.

In the case of bimetallic photocatalysts (Ag@(Au@TiO_2), Au@(Ag@TiO_2), Au&Ag@TiO_2; TiO_2=TIO-6), different abilities of methanol dehydrogenation depending on sequence of metal deposition were observed. The highest photoactivity showed photocatalyst in which gold was deposited on silver modified titania (Au@(Ag@TiO_2)). For this sample longer induction period (30 min) than in the case of monometallic gold photocatalyst (< 15 min), indicates that silver ions/NPs present on the surface of titania hinders gold reduction. Similarly, in the case of silver deposition on gold modified titania (Ag@(Au@TiO_2)), the induction period was also longer (45 min) than in the case of monometallic silver titania. The worst photocatalytic activity showed co-deposited sample (Ag&Au@TiO_2). It should be pointed out that only for this sample, the fastest hydrogen evolution occurred during first 15 min of deposition and then the process was almost negligible. This can suggest that simultaneous deposition of two metals causes preparation of specific bimetallic structures, *e.g.* alloys, which favour charge carriers recombination instead of charge separation. This is opposite to monometallic titania photocatalysts for which metallic deposits caused prolongation of charge carriers lifetime [10]. It must be pointed out that all bimetallic photocatalysts based on small rutile titania (TIO-6) showed much lower photo-reduction ability than monometallic ones indicating the possibilities of bimetallic nanostructures formation working as charge carriers recombination centres.

It is known that the formation of metallic NPs and evolution of hydrogen depend on physicochemical properties of the support [22]. The course of methanol dehydrogenation on bare and monometallic-modified rutile titania of large PPS (TiO_2=Ald_R, PPS=517 nm, BET=4 m^2g^{-1} [21]) is shown in Figure 1, right. Similarly to small rutile titania (TIO-6), gold

deposition on bare titania surface caused the fastest alcohol dehydrogenation, practically without the induction period. However, hydrogen evolution during deposition of monometallic silver NPs was the slowest. Successive deposition of metal on the surface of monometallic-modified titania proceeded after induction periods, shorter in the case of gold deposition on silver modified titania (8 and 16 min for Au@(Ag@TiO_2) and Ag@(Au@TiO_2), respectively; shown as dashed lines). It is worth noting that rates of hydrogen evolution in the case of these two bimetallic samples were almost the same (3.5 and 3.1 μmol min^{-1} for Ag@(Au@TiO_2) and Au@(Ag@TiO_2), respectively), suggesting that two metals were deposited independently on separate sites of titania surface. Hydrogen evolution was very slow during co-deposition of two metals (Ag&Au@TiO_2), similarly like in the case of small rutile titania, confirming the possibility of generation of bimetallic nanostructures, such as an alloy or core-shell, which acts as charge recombination centres. Gomez-Cortes *et al.* reported that Au and Ir co-deposition on Degussa P25 (commercial titania, 73-85% anatase, 14-17% rutile, 0-18% amorphous [23]) caused deposition of both metals only on rutile NPs, the same as in the case of monometallic Ir deposition, while successive deposition of gold on Ir@TiO_2 caused formation of metallic deposits on both titania forms independently [24]. It is thought that similarly in our case, successive deposition caused generation of individual metallic crystallites independently, while co-deposition led to formation of bimetallic nanostructures.

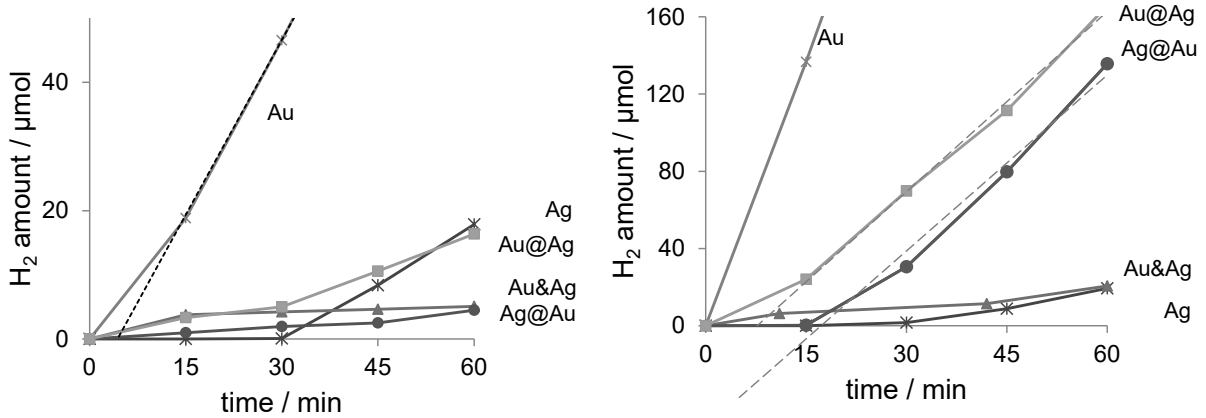

Fig. 1. Methanol dehydrogenation during photodeposition of noble metal NPs on rutile titania: TIO-6 (left) and Ald_R (right); Monometallic photocatalysts: Au (×), Ag (✳); Bimetallic photocatalysts: Au@Ag (■), Ag@Au (●), Au & Ag (▲).

Photodeposition was also carried out on the surface of anatase titania with large PPS (TiO_2=ST-41, PPS=208 nm, BET=11 m^2g^{-1} [21]). Obtained results were similar to data for large rutile NPs, *i.e.* the fastest and the slowest hydrogen evolution was observed for monometallic deposition of gold and silver, respectively. However, methanol dehydrogenation proceeded much faster on bimetallic photocatalysts when silver was deposited first on the support, *i.e.* 1.07 and 0.06 μmol min^{-1} for Au@(Ag@TiO_2) and Ag@(Au@TiO_2), respectively. Comparison of all photodeposition data, shown in Fig. 2 (left), indicates much higher photoactivity of monometallic gold titanias than monometallic silver- and bimetallic photocatalysts for hydrogen evolution. The larger cathodic currents observed for Au@TiO_2 than for Ag@TiO_2 has been already reported as a result of smaller overvoltage for H_2 evolution at an Au than an Ag electrode [25].

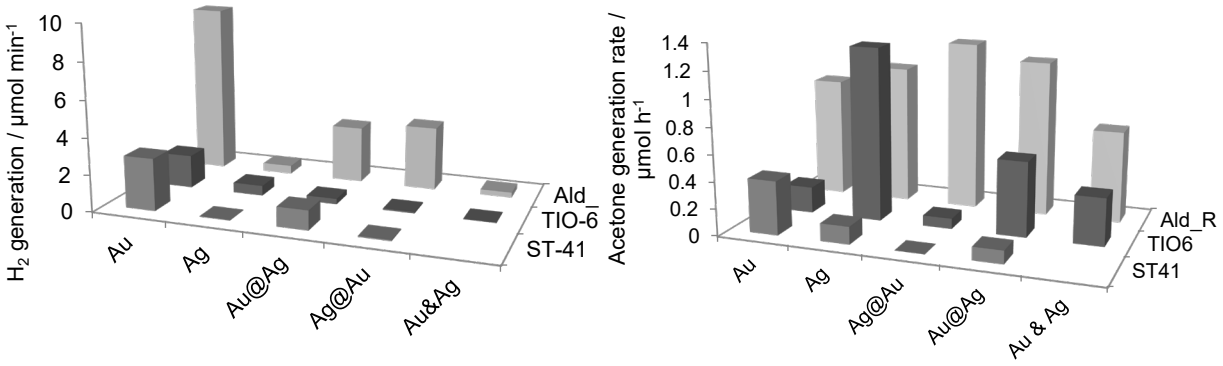

Fig. 2. Comparison of photocatalytic activity of plasmonic photocatalysts during methanol dehydrogenation under UV irradiation (left), and 2-propanol oxidation under visible light irradiation (>450 nm) (right).

3.2 Photocatalyst characterization

3.2.1 Crystalline composition

XRD analysis proved the deposition of gold and silver crystallites on Ald_R titania (Figure 3, top), and the presence of rutile as that main polymorphic form. It is worth noting that, due to almost the same position of silver and gold, *i.e.* 38.12° and 38.18°; 44.28° and 44.39°; 77.47° and 77.55° [26], respectively, it is impossible to distinguish them by XRD in the case of bimetallic photocatalyst. For monometallic modified titania of large PPS both silver and gold

could be easily detected by XRD. However, silver was undetectable when deposited on titania of small PPS (*e.g.* ST-01), suggesting that silver formed smaller NPs than gold (Figure 3, bottom). Recently, we have shown that size of generated gold NPs is directly proportional to the size of host titania NPs [13], and thus small gold NPs are formed on titania with small PPS. In the case of titania of small NPs the XRD peaks are very broad (Figure 3, bottom) and thus gold/silver and anatase titania overlapped for the most intense gold/silver peak, *i.e.* at 38°.

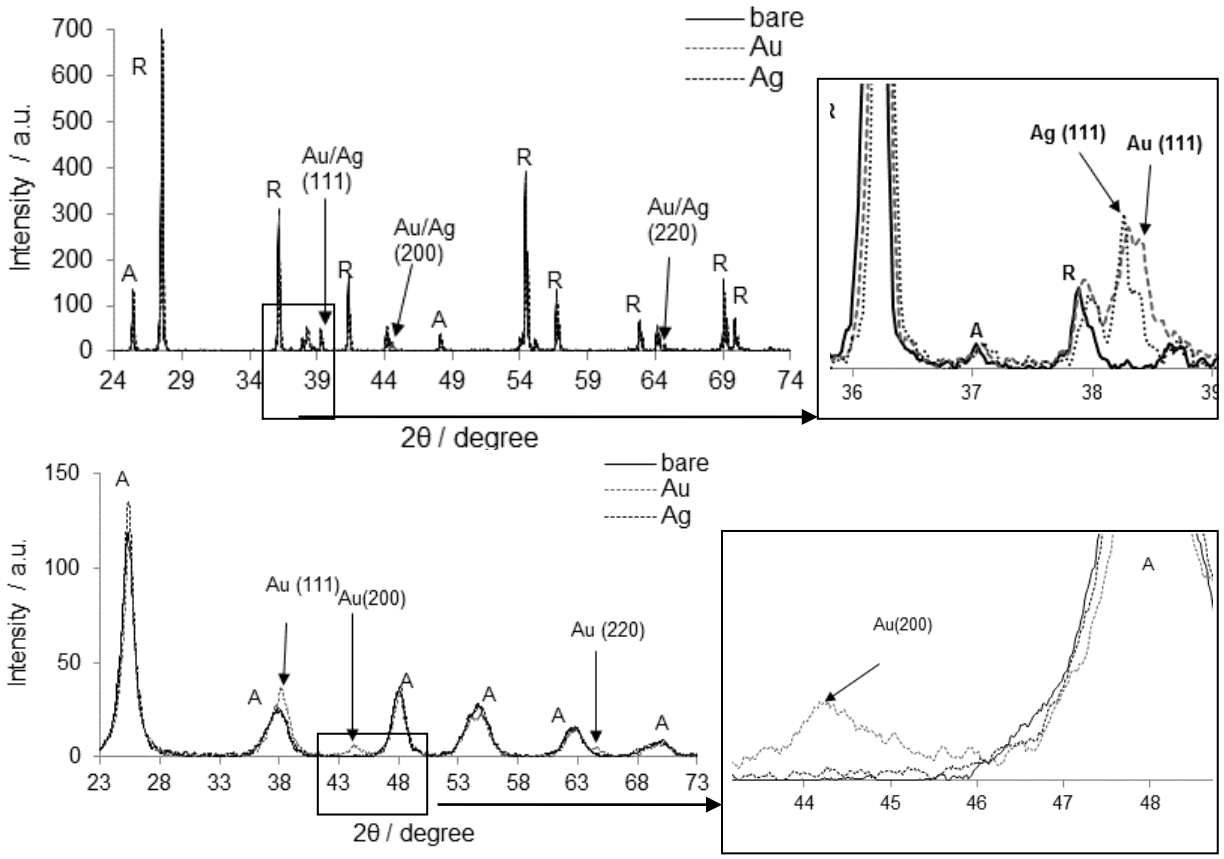

Fig. 3. XRD patterns of bare and monometallic modified titania: (top) Aldrich_R (Ald_R), (bottom) ST-01; Enlargement showing (111) facet of gold and silver and (200) facet of gold; R-rutile, A-anatase.

3.2.2 Atomic composition

Atomic composition and chemical characters of elements incorporated in the surface layer of modified titania have been investigated by XPS analysis. The presence of silver and gold was confirmed in all samples, and the amount of gold was much smaller than silver. The highest silver amount (3, 4.7 and 7 times higher than gold for Ald_R, TiO-6 and ST-41, respectively), obtained in the case of silver successive deposition on gold modified titania,

indicated the possibility of core(Au)-shell(Ag) formation. Successive gold deposition on silver modified titania resulted in increase of amount of gold. However the amount of silver was still much higher than gold (1.6, 2.6 and 5 for Ald_R, TiO-6 and ST-41) indicating preferential re-deposition of silver on gold surface than on titania. Co-deposition resulted in preparation of samples with almost the same silver to gold ratio (2.5-3) for all samples, suggesting formation of nanostructures reached in silver on the surface. Silver enriched surfaces have been already reported for nanocomposites prepared by microemulsion method [15]. It must be pointed that in the case of large rutile titania, the silver to gold ratios are the smallest suggesting that individual gold NPs should be also formed instead of bimetallic nanostructures.

The XPS analysis of Au 4f indicated the presence of $Au^{\delta-}$ (82.6 eV) and Au^0 (84.1 eV). The formation of $Au^{\delta-}$ caused by interaction between Au^0 and Ti^{3+} centers at crystallite defects in the titania has been previously reported [27]. The XPS spectra of Ag 3d indicated the presence of two or three components attributed to Ag^0 (368.3 eV), Ag^+ (Ag_2O, 367.6 eV) and Ag^{2+} (AgO, 367.05 eV) [15], where oxidized silver forms were predominant. It is thought that an electron enrichment of the Au surface atoms is caused by charge transfer from Ag to Au as was similarly observed for AuPt catalysts [28].

3.2.3 Absorption properties

All photocatalysts were coloured as a result of visible light absorption due to LSPR. The exemplary absorption spectra for large rutile titania: Ald_R are shown in Figure 4 (bottom, right). Usually, LSPR of silver is observed at shorter wavelengths than gold, *i.e.* for spherical NPs of 50-nm at 430 nm [29]. This indicates that either silver NPs larger than 50 nm were mainly formed or/and coupling between closely placed plasmonic structures occurred ("hot spots"). The simulation of LSPR for 50 nm silver NPs deposited on rutile titania indicated the presence of two plasmonic peaks at 430 nm (main peak) and at 560 nm (less intense) [29].

The broad silver LSPR peak indicates the variety of size and shape of deposited silver NPs. The absorption of gold modified titania was reported in our previous report, and three main

resonance peaks resulted from the presence of both spherical and rod-like gold NPs [14]. The rod-like NPs (nanorods, NRs) exhibited longitudinal (*ca.* 600 nm) and transverse (*ca.* 520 nm) LSPR. While absorption of nano-sized gold NPs was observed at much shorter wavelengths, *i.e.* 440 nm. In the case of bimetallic modified titania, one main LSPR peak was observed for successive deposition, while two separate peaks for simultaneous deposition (Au&Ag@TiO_2). It was reported that an existence of one LSPR peak placed between LSPR peaks of corresponding individual metals indicated that an Au-Ag alloy was formed, while for core(Au)-shell(Ag) NPs two characteristic absorbance peaks with bathochromic-shift of longitudinal LSPR was observed [30, 31]. One LSPR peak for core-shell structure [32], and the existence of two LSPR peaks for rod-like core(Au)-shell(Ag) NPs [33] were also reported. The existence of an alloy for Au@(Ag@TiO_2) and Ag@(Au@TiO_2) samples should be excluded, due to successive deposition [20], and thus either individual crystallites or composites structures, in which one metal can partly covered another, could be considered. It is expected that for core(Au)-shell(Ag) structures (Ag@(Au@TiO_2) the LSPR peak should have the same shape as LSPR of monometallic gold titania NRs (two plasmon resonance) [33]. Thus the existence of one broad peak suggested that two metals in the form of individual NPs of various size and shape were deposited on titania. The absorption shoulder at the shortest wavelengths corroborates presence of smaller nanoparticles, though, the main absorption/extinction spectral features are dominated by the largest volume nanoparticles. The strong bathochromic shift of main LSPR peak (*ca.* 690 nm) was observed for co-deposited sample (Au&Ag@TiO_2), confirming the expectation, based on methanol dehydrogenation (Figure 1, right), that Au/Ag composites were formed, probably in the form of core-shell. This is plausible due to close values of the lattice constants of Au (0.409 nm) and Ag (0.40788 nm) which are only 0.27% different. The existence of another LSPR peak at much shorter wavelengths (*ca.* 490 nm, even shorter than for monometallic silver modified titania) may suggested that an alloy or core-shell based on nanosized NPs was also formed. However, due to variety in size and shape of

generated NPs (as shown in Fig. 4) it is difficult to match unequivocally LSPR peaks as an alloy, composite nanostructure or individual NPs.

3.2.4 Distribution of metal NPs

Microscopic observation confirmed the existence of gold NPs of various sizes and shapes, as well as rod-like NPs (Figure 4, top). In the case of monometallic silver deposition, the presence of large (> 70 nm) and nano-sized (*ca.* 1-2 nm) silver NPs was detected (Figure 4,

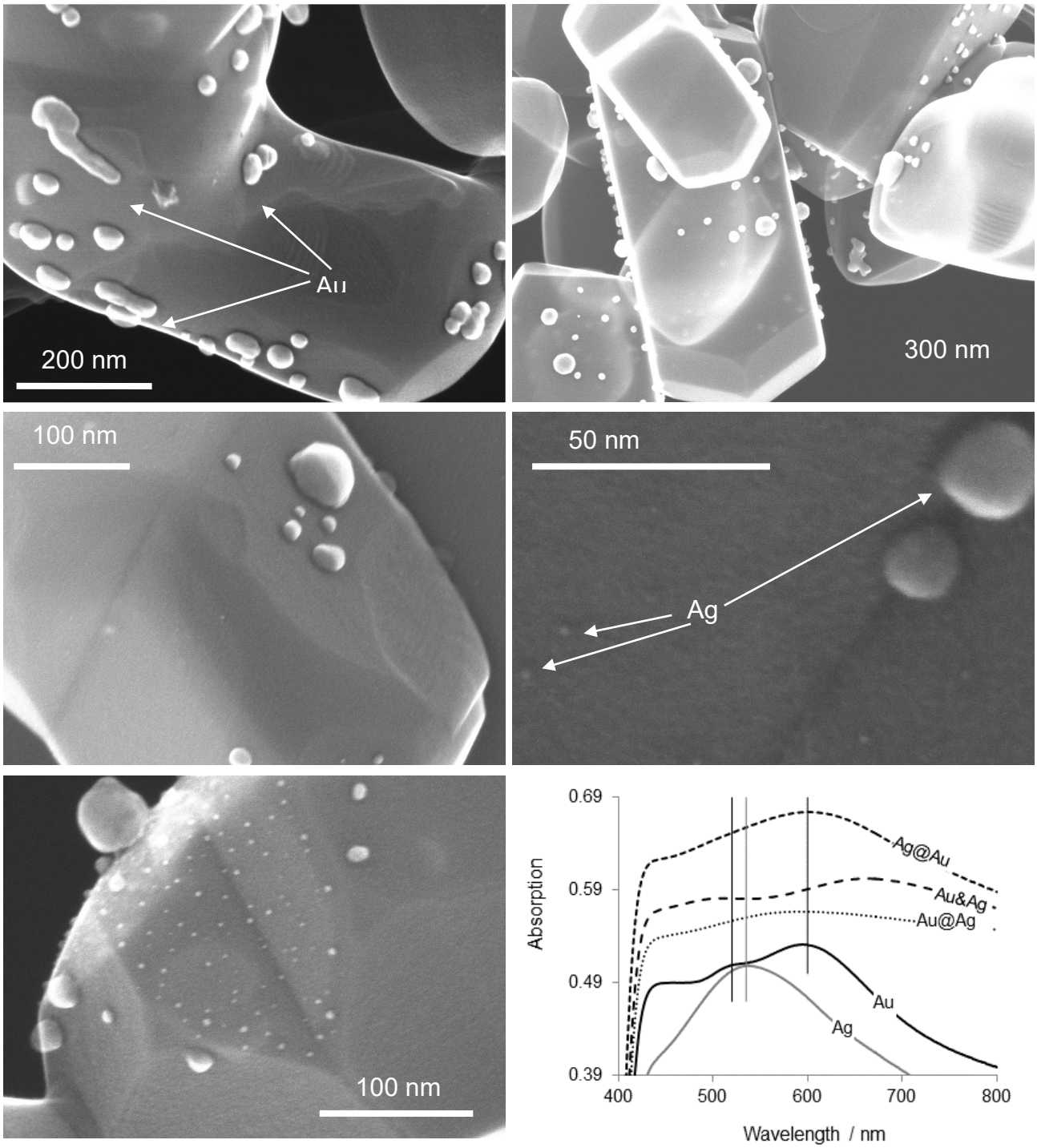

Fig. 4. STEM of monometallic- and bimetallic-modified rutile titania (Ald_R): Au@TiO_2 (top), Ag@TiO_2

(middle), Ag@(Au@TiO_2) (bottom, left), and DRS of Ald_R rutile titania (bottom, right)

middle). While, for bimetallic modified titania, the smallest metallic NPs were a little larger than in the case of silver monometallic-modified titania (Figure 4, bottom). However, it is impossible to distinguish whether these NPs were in the form of alloys or individual metallic NPs. To prove the form of metallic deposits an EDS mapping is presently performed.

3.3 Photocatalytic activity under visible light irradiation

The visible activities of monometallic- and bimetallic-modified titanias are shown in Figure 2, right. Silver deposition on the surface of rutile titania photocatalysts (TIO-6 and Ald_R) caused the highest level of activity. The higher photoactivity of silver than gold modified titania have been already reported for dye degradation under UV irradiation [34]. Bimetallic photocatalysts on small rutile (TIO-6) and on large anatase (ST-41) titanias exhibited much lower photoactivity than respective monometallic samples. Recently, deactivation of titania photocatalysts after modification with an alloy of Au-Cu under visible light irradiation have been also reported [17]. The enhancement of photoactivity was observed for large rutile titania (Ald_R) when second metal was successively deposited on the surface of monometallic-modified titania, in contradiction with literature expectation that bimetallic NPs obtained by successive deposition, and thus in the other form than alloys, were not interested for photocatalytic application [20]. It is important noting that previously the other role of metallic deposits was considered, such as inhibition of recombination of photo-generated charge carriers (e^-/h^+) under UV irradiation of titania. While presently noble metal NPs activating titania under visible light irradiation by LSPR are under study. An advantage of successive deposition over co-deposition has been recently reported for titania modified with Au and Ir for dark catalytic reactions [24].

3.4 Simulation of LSPR for bimetallic titania

To examine the influence of the presence of second metal (bimetallic composites) on LSPR position and on its intensity, the theoretic simulation for bimetallic Ag@Au NPs deposited on

titania was performed. The results for 10 x 10 x 30 nm spheroidal gold NPs covered with 2 or 5 nm-sized of silver layer, and deposited on titania surface are shown in Figure 5. The absorption (dashed lines) and extinction (solid lines) peaks overlapped since scattering for such small NPs was negligible. The position of LSPR peak depended on the presence of silver layer and its thickness. In the model with no cover, extinction peaks was at 510 nm, and the extinction cross-section had a maximum value of 100 nm^2. When the particle was covered by a thin silver layer of 2 nm thickness, the peak extinction cross-section was increased by 70% and bathochromic-shifted to 600 nm. When the layer thickness was increased to 5 nm, the cross-section peak was slightly shifted to 570 nm and one order of magnitude larger than the uncovered case. The most similar experimental LSPR spectrum was observed for co-deposited sample (Figure 4, right bottom), in which strong bathochromic-shift was observed from 605 (for monometallic Au@TiO_2) to 680 nm, indicating the possibilities of Ag@Au core-shell formation on the surface of titania.

The intensity enhancement patterns (the inset of Figure 5) show field distribution depending on silver presence. For uncovered gold NP a symmetrical distribution of the intensity enhancement with side hot-spots and a maximum enhancement of 13 was noticed (top inset). For gold NP covered with 2-nm silver layer (middle inset), a single wide hot-spot was formed at the interface with the titania substrate, spanning the width of the cover, and the maximum enhancement of 3100 was found at the tip of the gold spheroid (interface titania/gold). While for 5-nm silver layer the strongest enhancement (bottom inset) was observed as the hot-spot separated in different enhancement zones at the tip of the gold spheroid (with its maximum equalled 10000) and at the corners of the silver cover. The enhancement of field for bimetallic NP could indicate the higher level of photoactivity than that for monometallic NP, especially that field enhancement was observed at the interface between titania and NP. However, higher ability of charge generation at the interface does not mean higher photoactivity, since plasmonic electrons instead of being transferred from silver to CB

(conduction band) of titania may sink in nearby gold NP and *vice versa*, as shown in Fig 5, right. Indeed, plasmonic metals can be excited at visible wavelengths via d-to-sp band transitions, recombining upon relaxation; once there is a pair of metals the relaxation is expected to be more efficient due to larger available density of electronic states. Thus, observable inhibited photoactivity of co-deposited metals could be cause by this mechanism. Recently, an electron transfer from gold to platinum for Pt-Au bimetallic alloys has been reported [28].

Two main mechanisms for plasmonic titania photocatalysts under visible light irradiation have been considered, *i.e.* i) charge carrier transfer (electron transfer from plasmonic metal NPs to CB of titania [11, 13, 35]), and ii) energy transfer (from plasmonic NPs to titania [12, 18]). Present results, showing activity loss for bimetallic titania photocatalysts, could prove the charge transfer mechanism as the main mechanism in our system, since it is expected that for energy transfer mechanism the improvement of photocatalytic reaction should be observed with field enhancement.

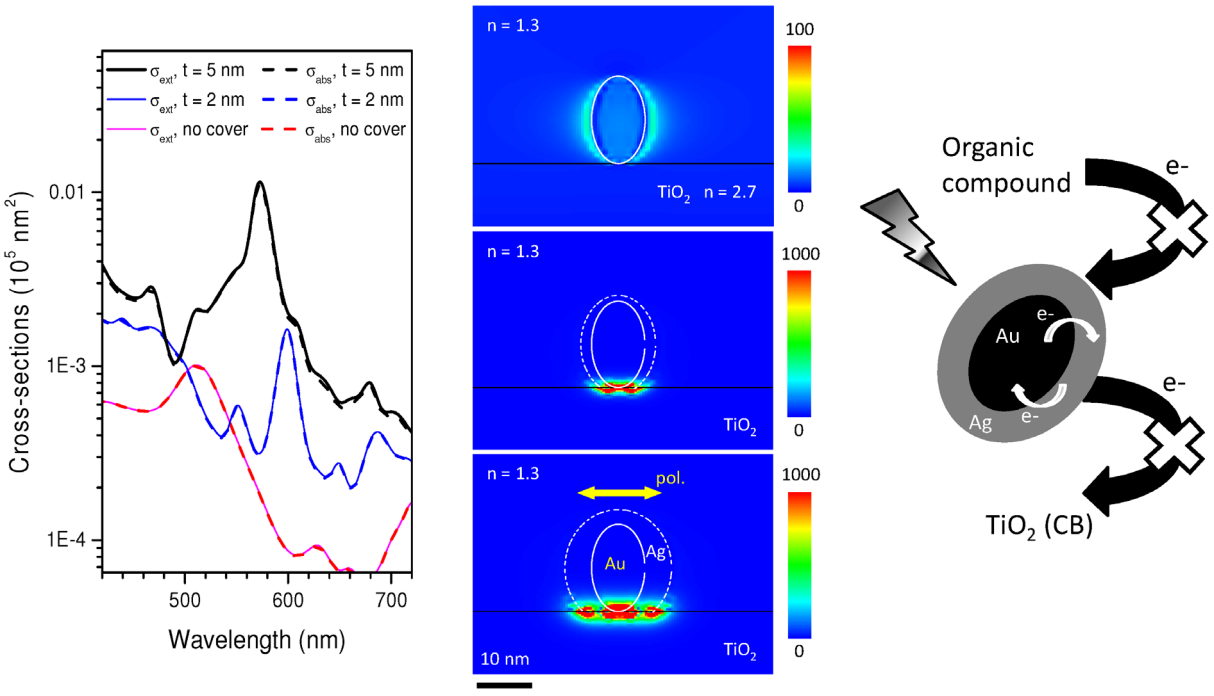

Fig. 5 (left) Dependence of extinction (σ_{ext}, solid lines) and absorption spectra (σ_{abs}, dashed lines) of 10 x 10 x 30 nm spheroidal gold NP on the presence of coverage layer of silver of thickness t; (center) The cross-sectional pattern of the near-field intensity enhancement factor for (top) t=0 at 510 nm wavelength, (middle) t=2 nm at 600 nm, (bottom) t=5 nm at 570 nm; n-refractive index; (right) Schematic representation of inhibition of OCs oxidation

on titania modified with bimetallic core-shell NP.

4. Conclusions

Photoactivity of plasmonic titania photocatalysts depends on properties of titania and noble metal NPs. Gold monometallic photocatalysts exhibited much higher activity during alcohol dehydrogenation under UV irradiation than silver monometallic and Au/Ag bimetallic photocatalysts. On the contrary, under visible light oxidation of 2-propanol, monometallic silver titania showed much higher photoactivity than gold ones. Different function of noble metal NPs for different irradiation ranges, *i.e.* a sink of photogenerated electrons resulting in lower charge carriers recombination (higher activity) and light harvesting under UV and visible light irradiation, respectively, could be responsible for such behaviour. The photoactivity of bimetallic Au-Ag photocatalysts under visible light irradiation depends on titania source. Photocatalysts obtained by photodeposition of bimetallic NPs on titania with smaller NPs (TIO-6, ST-41) lost the photoactivity independently on the kind of deposition, *i.e.* successive or co-deposition. While, photocatalysts obtained by successive and simultaneous photodeposition on titania with large PPS (Ald_R) showed improved and reduced photoactivity, respectively. It is thought that successive deposition allowed preparation of photocatalysts with individually deposited monometallic NPs of various size and shape, and thus with ability of light absorption at broad wavelength ranges. While, co-deposition resulted in formation of bimetallic composites, *e.g.* alloys, core-shell structures, in which plasmonic photo-generated electrons sank into nearby second metal, instead of being transferred to CB of titania. Numerical simulation showed that core/Au-shell/Ag structures exhibited enhanced field at the interface between titania and metallic NP. This data suggest electronic rather than energy transfer mechanism for plasmonic photocatalysts under visible light irradiation.

Acknowledgements

This research was funded by a grant from Bill & Melinda Gates Foundation through the Grand Challenges Explorations initiative (GCE R8, OPP1060234).

References

[1] R.E. Smalley, Nanotechnology, Energy and People, MIT Forum, River Oaks, USA, 2003.
[2] M. Primet, P. Pichat, M.-V. Mathieu, J. Phys. Chem. 75 (1971) 1216-1220.
[3] A.L. Pruden, D.F. Ollis, J. Catal. 82 (1983) 404-417.
[4] S. Nishimoto, B. Ohtani, H. Kajiwara, T. Kagiya, J. Chem. Soc. 79 (1983) 2685-2694.
[5] M. Barbeni, E. Pramauro, E. Pelizzetti, E. Borgarello, M. Grätzel, N. Serpone, Nouv. J. Chim. 8 (1984) 547-550.
[6] R. Asahi, T. Morikawa, T. Ohwaki, K. Aoki, Y. Taga, Science 293 (2001) 269-271.
[7] S. Sakthivel, M. Janczarek, H. Kisch, J. Phys. Chem. B 108 (2004) 19384-19387.
[8] W. Choi, A. Termin, M.R. Hoffmann, J. Phys. Chem. 98 (1994) 13669-13679.
[9] P. Pichat, J.M. Herrmann, J. Disdier, H. Courbon, M.N. Mozzanega, Nouv. J. Chim. 5 (1981) 627-636.
[10] E. Kowalska, H. Remita, C. Colbeau-Justin, J. Hupka, J. Belloni, J. Phys. Chem. C 112 (2008) 1124-1131.
[11] Y. Tian, T. Tatsuma, J. Am. Chem. Soc. 127 (2005) 7632-7637.
[12] P.A. DeSario, J.J. Pietron, D.E. DeVantier, T.H. Brintlinger, R.M. Stroud, D.R. Rolison, Nanoscale 5 (2013) 8073-8083.
[13] E. Kowalska, R. Abe, B. Ohtani, Chem. Commun. (2009) 241-243.
[14] E. Kowalska, O.O.P. Mahaney, R. Abe, B. Ohtani, Phys. Chem. Chem. Phys. 12 (2010) 2344-2355.
[15] A. Zielińska-Jurek, E. Kowalska, J.W. Sobczak, W. Lisowski, B. Ohtani, A. Zaleska, Appl. Catal. B: Environ. 101 (2011) 504-514.
[16] M. Jakob, H. Levanon, P.V. Kamat, Nano Lett 3 (2003) 353-358.
[17] Z.B. Hai, N. El Kolli, D.B. Uribe, P. Beaunier, M. Jose-Yacaman, J. Vigneron, A. Etcheberry, S. Sorgues, C. Colbeau-Justin, J.F. Chena, H. Remita, J Mater Chem A 1 (2013) 10829-10835.
[18] D.B. Ingram, P. Christopher, J.L. Bauer, S. Linic, Acs Catal 1 (2011) 1441-1447.
[19] E. Kowalska, S. Rau, B. Ohtani, Journal of Nanotechnology 2012 (2012) 1-11.
[20] J.M. Herrmann, J. Disdier, P. Pichat, A. Fernandez, A. Gonzalez-Elipe, G. Munuera, C. Leclercq, J. Catal. 132 (1991) 490-497.
[21] O.O. Prieto-Mahaney, N. Murakami, R. Abe, B. Ohtani, Chem. Lett. 38 (2009) 238-239.
[22] B. Ohtani, Y. Okugawa, S. Nishimoto, T. Kagiya, 91 (1987) 3550-3555.
[23] B. Ohtani, O.O. Prieto-Mahaney, D. Li, R. Abe, J Photoch Photobio A 216 (2010) 179-182.
[24] A. Gomez-Cortes, G. Diaz, R. Zanella, H. Ramirez, P. Santiago, J.M. Saniger, J. Phys. Chem. C 113 (2009) 9710-9720.
[25] G. Zhao, H. Kozuka, T. Yoko, 277 (1996) 147-154.
[26] D. Barthelmy, Mineralogy database, 2009.
[27] M.S. Chen, D.W. Goodman, Accounts Chem Res 39 (2006) 739-746.
[28] R.P. Doherty, J.-M. Krafft, C. Methivier, S. Casale, H. Remita, C. Louis, C. Thomas, J. Catal. 287 (2012) 102-113.
[29] V. Mizeikis, E. Kowalska, S. Juodkazis, J. Nanosci. Nanotechnol. 11 (2011) 2814-2822.
[30] M.P. Mallin, C.J. Murphy, Nano Lett. 2 (2002) 1235-1237.
[31] L. Rivas, S. Sanchez-Cortes, J.V. Garcia-Ramos, G. Morcillo, Langmuir 16 (2000) 9722-9728.
[32] H. Han, Y. Fang, Z. Li, H. Xu, Appl. Phys. Lett. 92 (2008) 023116-023111-023113.
[33] C.S. Ah, S.D. Hong, D.-J. Jang, J. Phys. Chem. B 105 (2001) 7871-7873.
[34] W. Liang, T.L. Church, A.T. Harris, Green Chem. 14 (2012) 968-975.
[35] L. Du, A. Furube, K. Hara, R. Katoh, M. Tachiya, Thin Solid Films 158 (2009) 861-864.